Journal of Power Sources 253 (2014) 224–229

Contents lists available at ScienceDirect

Journal of Power Sources

journal homepage: www.elsevier.com/locate/jpowsour

Detecting and localizing failure points in proton exchange membrane fuel cells using IR thermography

Guido Bender*, Wyatt Felt, Michael Ulsh

National Renewable Energy Laboratory, 15013 Denver West Parkway, Golden, CO 80401, USA

HIGHLIGHTS

- We present a novel diagnostic hardware for IR thermography studies on PEMFCs.
- We detect failure points that developed in MEAs after accelerated stress tests.
- We detect failure points that developed at electrode coating irregularities.
- Our method is valuable for determining the most stressed areas within an MEA.

ARTICLE INFO

Article history:
Received 19 August 2013
Received in revised form
6 December 2013
Accepted 9 December 2013
Available online 18 December 2013

Keywords:
Fuel cell
PEMFC
Durability
Thermography
Failure
Accelerated stress test

ABSTRACT

An understanding of the potentially serious long-term performance degradation effects that coating and/or other fabrication irregularities might have in mass produced proton exchange membrane fuel cells (PEMFC) is essential to determine manufacturing tolerances of fuel cell components. An experimental setup and methodology is described that employs accelerated stress tests (ASTs) and IR thermography to accurately determine the location and severity of developing failure points in PEMFCs. The method entails a novel hardware that allows the spatial observation of a hydrogen crossover experiment within a fuel cell hardware. The application of the method is demonstrated by comparing the effects of an AST on pristine as well as defect-containing MEAs. The presented method is shown to be valuable for determining the areas within a fuel cell that are most stressed by aging processes.

1. Introduction

Polymer electrolyte membrane fuel cells (PEMFCs) are energy conversion devices that offer high power densities at low operating temperatures making PEMFCs the most promising technology for many applications such as automobiles, back-up power generating units, and portable devices. While design and material considerations for PEMFCs have a large impact on cost, it is also necessary to consider a transition to high volume production of fuel cell systems, including membrane electrode assembly (MEA) components, to enable economies of scale and reduce per-unit cost. The fuel cell industry has identified quality control as a critical barrier for continuous production of MEA components, i.e. membranes, electrodes, and GDLs. One of the critical manufacturing tasks is developing and deploying techniques to provide in-process measurement of fuel cell components for quality control. This work focuses on a necessary subsidiary task: The study of the effect of manufacturing defects on performance and durability with the objective to establish validated manufacturing tolerances for fuel cell components.

The durability of fuel cell materials including catalyst layer, ionomer, and other MEA components has gained increasing attention since it remains one of the barriers that need to be overcome to successfully place fuel cells in the market place. The need for improving and understanding the durability of fuel cell components and materials is reflected in the increasing magnitude of recent publications on this topic as shown in Borup et al.'s comprehensive literature review from 2007 on fuel cell durability and degradation [1]. The review organized the reported work in chapters for operational effects on fuel cell durability, membrane degradation, electrocatalyst stability, and gas diffusion layers. Another detailed and extensive resource on fuel cell degradation is the book by Mench et al., in 2012. They address in their chapters

* Corresponding author. Tel.: +1 (303) 275 3810.
E-mail address: guido.bender@nrel.gov (G. Bender).

0378-7753/$ – see front matter © 2013 Elsevier B.V. All rights reserved.
http://dx.doi.org/10.1016/j.jpowsour.2013.12.045

membrane durability; electrochemical, gas diffusion media, and bipolar plate degradation; and freeze damage; as well as current status and targets of durability, experimental diagnostics and test protocols, high resolution characterization techniques for degradation studies in fuel cells, and computational aspects of PEFC durability [2]. More recent work also focused mostly on operation induced degradation of the various functional layers and materials within a fuel cell. Reports include the development of catalyst layer cracks due to humidity cycling [3], degradation effects due to vehicle operation [4], degradation of Nafion with various thicknesses in the same stack [5,6], effects of open circuit operation [7], and durability test protocols [8].

One aspect of PEMFC durability which, to date, has been entirely overlooked is the effect that production quality control thresholds may have on the durability of fuel cell. This work is a first step toward closing this deficiency. We are presenting the development and demonstrating the feasibility of a diagnostic tool and methodology that allow for the quasi in-situ spatial detection of failure points in a single cell PEMFC.

2. Experimental

Experiments were performed at the National Renewable Energy Laboratory (NREL) using a fully calibrated fuel cell test station from Fuel Cell Technologies, Inc. Pristine and defect-containing membrane electrode assemblies (MEAs) of 50 cm^2 size were manufactured in-house by ultrasonically spraying Pt containing catalyst ink on ethylene tetrafluoroethylene (ETFE) decal material. The catalyst ink contained 49.5wt% Pt/C catalyst from Tanaka, 20wt% Nafion® solution with 1100 EW from Ion Power, de-ionized water, and *n*-propanol. The Nafion®/carbon weight ratio of the ink was adjusted to 0.8. Subsequent to spraying, the catalyst layers were transferred via a hot press transfer step onto proton form Nafion® NRE212 membrane using a temperature of 135 °C, and a pressing duration of 5 min. During hot pressing the Nafion® was sandwiched between (i) the catalyst layer-supporting ETFE decals, (ii) 2 mil thick Kapton sheets, and (iii) Gylon sheets. A compression force of 31 kg cm^{-2} was applied; the total force was calculated with respect to the size of the Gylon sheets. MEAs with artificially induced cathode electrode coating defects were created by masking off a square area of 2 cm^2 size near the center of the electrode during the ultrasonic spray process. As shown in Fig. 1, this created a 100% catalyst loading reduction of defined size, geometry, and location.

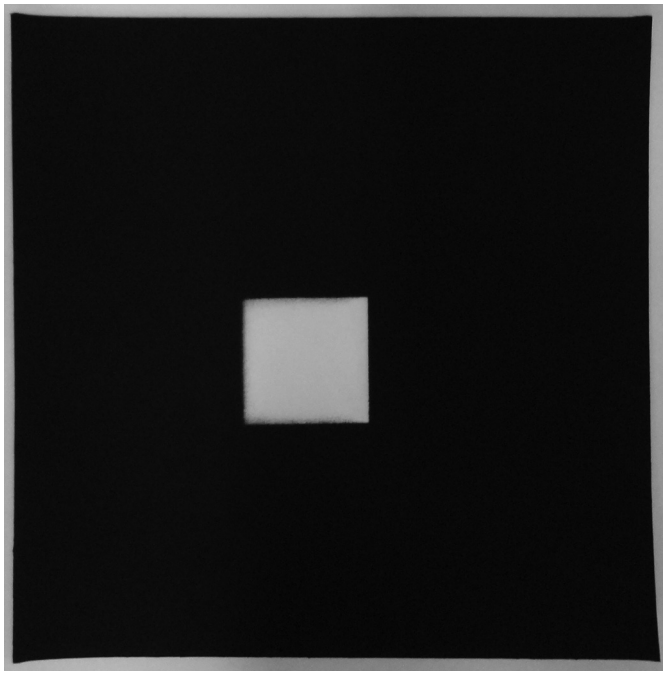

Fig. 1. ETFE decal holding an ultrasonically sprayed 50 cm^2 electrode that contained a 2 cm^2 100% catalyst loading reduction defect, i.e. the white uncoated area.

Table 1
Test conditions for accelerated stress tests.

AST conditions	
AST duration until OCV test	24 h
Cell temperature	80 °C
H_2/air gas flows	2000/2000 sccm
Pressures	150/150 kPa
Humidification	90/90 and 20/20 °C dew points switching every 2 min

The resulting pristine and defect-containing catalyst coated membranes (CCMs) were assembled with Sigracet 25-BC gas diffusion media (GDL) using Polytetrafluoroethylene (PTFE) gaskets. Gasket thickness was chosen to establish 20% GDL compression while assuming 6% gasket compression at a compression torque of 40 inch pounds. All cells were conditioned at 80 °C using NREL's standard conditioning procedure which includes cell voltage cycling between 0.85 and 0.6 V for 5 and 10 min, respectively, over a total of 20 cycles.

Accelerated stress tests (ASTs) were performed combining the DOE recommended protocols for mechanical and chemical stability. The test conditions, which are summarized in Table 1, consisted of exposing the anode/cathode electrodes of the MEA to 2000/2000 sccm H_2/air gas flows at a cell temperature of 80 °C and open circuit voltage (OCV) over extended periods of time. Additionally, as shown in Fig. 2, gas humidity conditions were alternated every 2 min from a dew point of 90 °C to approximately 20 °C by passing the humidifier bottle of the anode and cathode gas streams. Between each aging period, the open circuit voltages (OCV) at 0, 2, and 4 psi differential pressure between anode and cathode electrode were determined as shown in equation Eq. (1).

$$\Delta p = p_{\text{anode}} - p_{\text{cathode}} \tag{1}$$

The outcome of these experiments were used as an indicator for the development of failure points in the MEA, i.e. a decreasing OCV

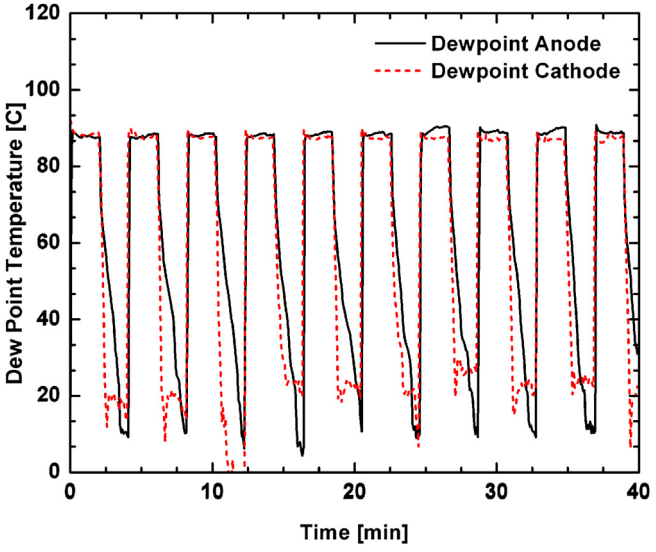

Fig. 2. AST combining DOE AST for mechanical and chemical membrane degradation.

at $\Delta p > 0$ indicated the development of a failure point; the more the OCV declined, the further developed is the failure point. Upon detection of any failure point development, further exposure to the AST was terminated.

3. Hardware and principle of thermography experiments

Infrared thermography has received growing attention as a nondestructive diagnostic technique in the last few decades, due to dramatic technological improvements and relative cost reductions of IR cameras [9]. This trend is reflected in the development of IR based diagnostics for PEMFCs, which include thermography mapping for electrical shorts [10], heat produced during fuel cell operation [11], and membrane perforation [12]. Given its sensitivity, high resolution, and simplicity of use, IR thermography is also an obvious choice for quality control diagnostic devices for fuel cell components. NREL has demonstrated its feasibility for 100% areal inspection of moving fuel cell material at currently typical production speeds in previous work [13–15]. IR thermography is further valuable for research on MEA durability as demonstrated by Yuan et al., who used the technique for the ex-situ analysis of membrane material before and after exposure to a degradation period [5,7,16]. In this work we present the development of a low cost PEMFC hardware that allows for regular fuel cell operation as well as quasi in-situ spatial hydrogen crossover experiments via IR thermography. This hardware thus allows combining the inducement of aging processes via regular operation or accelerated stress tests with the spatial observation of developing failure points in the same device.

The cathode endplate, current collector plate, and flow-field of a 50 cm^2 single cell hardware were redesigned to enable the spatial detection of failure points in a PEMFC by means of IR thermography. The resulting *IR hardware* is shown in the exploded view of Fig. 3. The figure shows from left to right: a standard endplate, a standard current collector plate, a standard flow-field, a GDL, a gasket, a CCM, a gasket, a GDL, an anodized aluminum “hardware frame”, and a gold-plated aluminum “flow-field insert”. Both aluminum parts can be assembled to each other with a set of bolts. When assembled, the flow-field insert and frame offered the functionality of a standard cathode hardware part. The flow-field block provided the gas in- and outlet, the flow-field, part of the sealing surface, the temperature control port, and a surface to attach a heat source. The aluminum frame further provided holes for CCM, gasket, and hardware alignment, the main sealing surface, and the bolt locations for hardware assembly with the anode part of the hardware, i.e., a fuel cell assembly with CCM, GDLs and gaskets.

Such an assembly is shown as a cross-sectional diagram and a picture in Fig. 4(a) and (b). In this *fuel cell configuration* the cell could be operated as a typical research-scale single cell fuel cell. Pressures, gas flows, temperature, gas humidification, and cell current or voltage could be controlled as required for the desired experiment. When stopping the gas flows and removing the flow-field insert from the assembly, the fuel cell hardware was switched to its *IR configuration*. This configuration of the hardware allowed the interrogation of the MEA via IR thermography as shown in the cross-sectional diagram and picture of Fig. 5(a) and (b). In contrast to ex-situ IR thermography hardware developed to probe for MEA perforation in a post-mortem analysis step [16], the presented hardware enabled aging the cell using a repeated in-situ procedure of defined duration, while probing for the development of failure points in between aging steps. Further, the objective to monitor the spatial hydrogen crossover in the same hardware but separate from a performance experiment allowed for a simple and straightforward hardware solution. The hydrogen crossover experiment could be performed at ambient conditions, which eliminated the need of integrating an IR transmissive material window into the flow-field and endplate section. In *IR configuration*, the cathode flow-field was removed from the hardware and the electrode was exposed to the environment, i.e., approximately 21% oxygen in nitrogen balance at room temperature. The aluminum frame remained tightly attached to the anode endplate, maintaining the seal of the anode compartment and keeping the MEA aligned and in place. To perform IR thermography an IR camera (Jenoptic, HiRes) was placed in front of the exposed cathode-side of the MEA.

When flowing small flows of hydrogen or hydrogen/inert mixtures, any hydrogen diffusing across the MEA would cause an exothermic reaction with the ambient oxygen. Since elevated hydrogen amounts were present at locations of membrane thinning, pinholes, or failure point development, the method was expected to allow for the detection of such locations.

4. Results and discussion

The described hardware and AST procedure was employed to demonstrate the localization and detection of failure points in MEAs. Fig. 6(a) shows the pristine MEA: (i) the OCV during MEA exposure to the AST (gray line) and (ii) distinct OCV experiment at 0, 2, and 4 psi differential anode/cathode pressure (symbols) during which the AST was interrupted. The AST in Fig. 6(a) was interrupted and restarted at 18 h and stopped after 56 h. The data indicate that the AST resulted, as expected, in a continuous degradation of the open circuit voltage. From starting to end of the AST the OCV

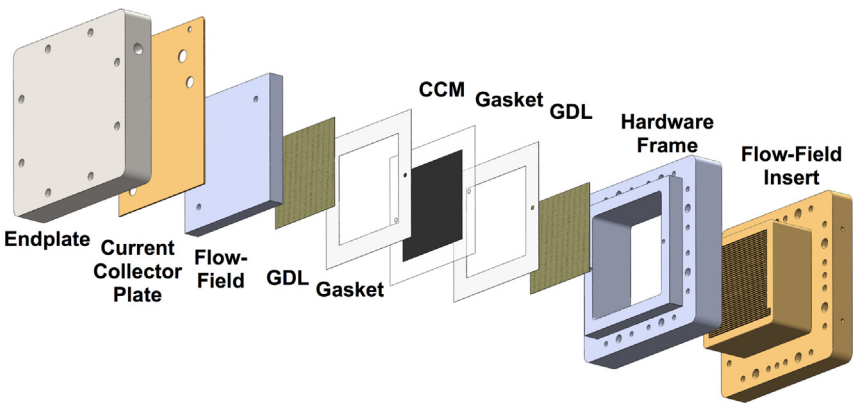

Fig. 3. Fuel cell hardware for IR thermography.

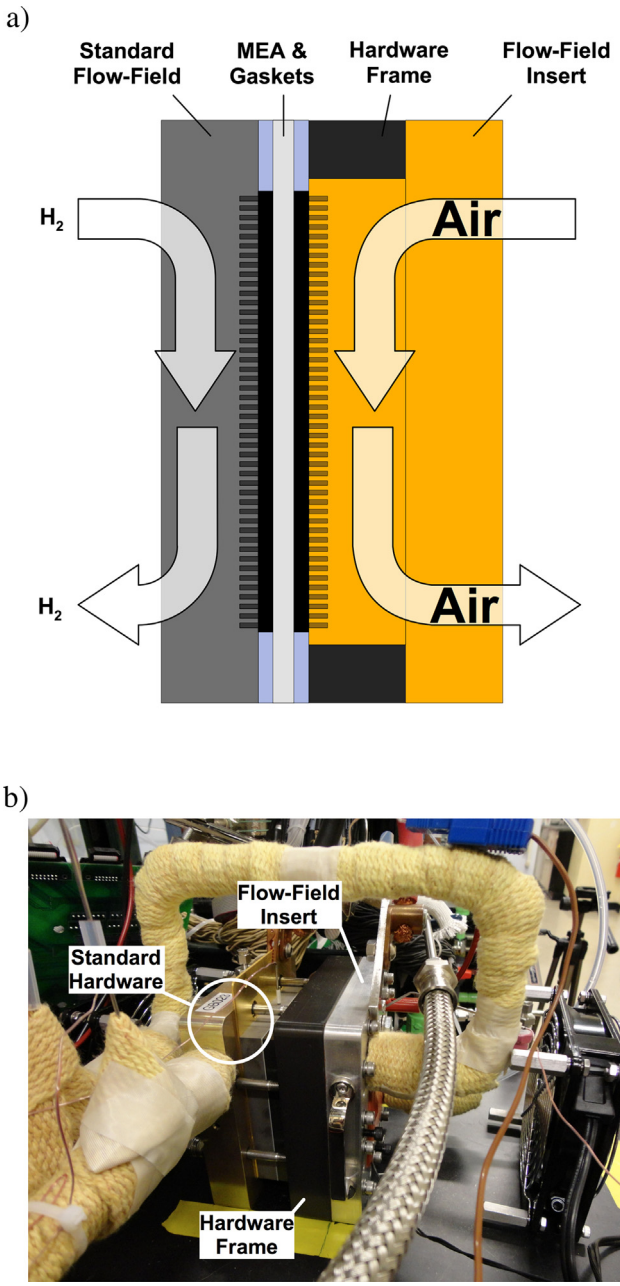

Fig. 4. Fuel cell mode (a) schematic, (b) picture of IR hardware.

dropped by 90 mV from 971 mV to 881 mV. This reduction of the OCV is typical for PEMFC and an indicator for MEA degradation. To date, its cause is not fully understood and is subject to ongoing research [17–20]. The data in Fig. 6(a) also indicated that after 18 h of exposure to the AST, the OCV was insensitive to pressure changes regardless of applying a differential pressure. Please note that the initial two sets of differential pressure OCV experiments were performed using lower gas dew point temperatures of 80/80 °C for both, anode and cathode, respectively, while all other differential pressure OCV experiments were performed with dew points of 90/90 °C. However, the results indicated that the MEA was still intact. After 56 h, a 55 mV drop of the OCV was observed when applying a 2 psi positive pressure differential Δp from the anode to the cathode, and a 82 mV drop when applying 4 psi, respectively. This change in OCV with Δp indicated that a failure point had developed in the MEA.

Similar results were observed for an MEA that contained a 2 cm^2 defect, as shown in Fig. 6(b). Over the course of the AST the OCV of this MEA degraded by 99 mV. After 24 h of exposure to the AST, the OCV was insensitive to pressure changes regardless of applying a differential pressure. This indicated that the MEA was still intact. However, after 48 h, the OCV dropped by 391 mV when exposed to a pressure differential of 2 psi. This indicated the development of a failure point between 24 and 48 h. Please note that upon measuring the high OCV change at $\Delta p = 2$ psi the measurement at $\Delta p = 4$ psi became obsolete and was not conducted to avoid physical damage to the MEA.

For both cases shown in Fig. 6(a) and (b), AST exposure was stopped, the gas flows interrupted, and the hardware converted from *fuel cell configuration* to *IR configuration*. Fig. 7(a) and (b) shows IR thermography results for the pristine MEA after 18 and 56 h of AST exposure, respectively. The colors in the IR images represent temperature values between 22 °C (dark blue) and 59.6 °C (red/white).

The data indicate that the MEA was fully intact after 18 h of aging, while after 56 h a hole had developed at the right edge of the active area, between catalyst layer/GDL and gasket. This transition

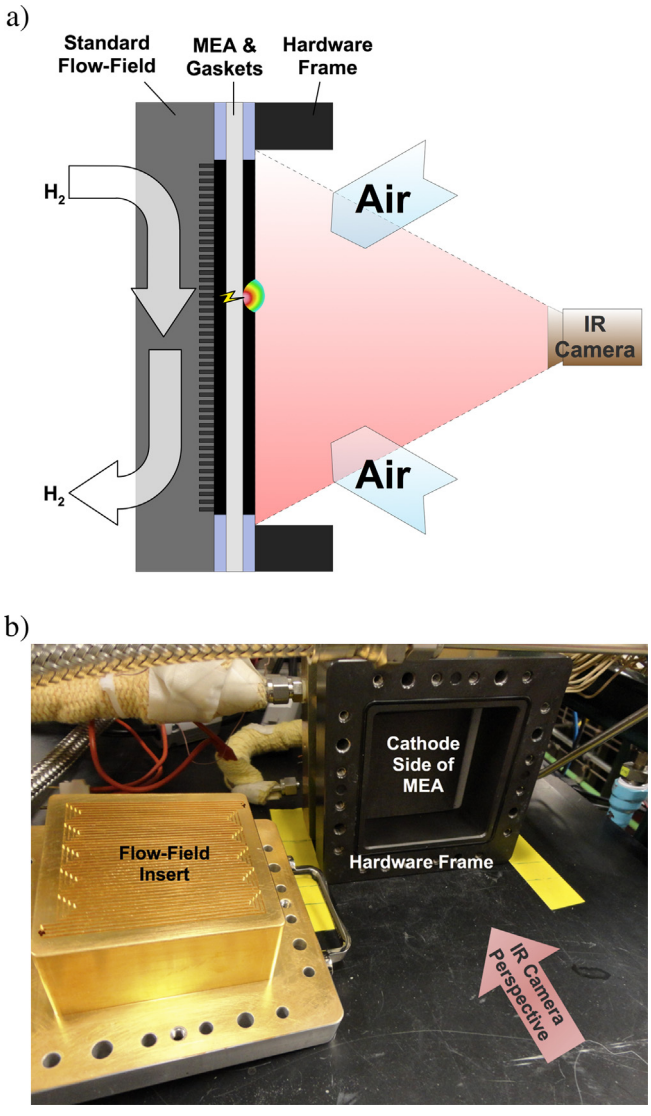

Fig. 5. IR thermography mode (a) schematic, (b) picture of IR hardware.

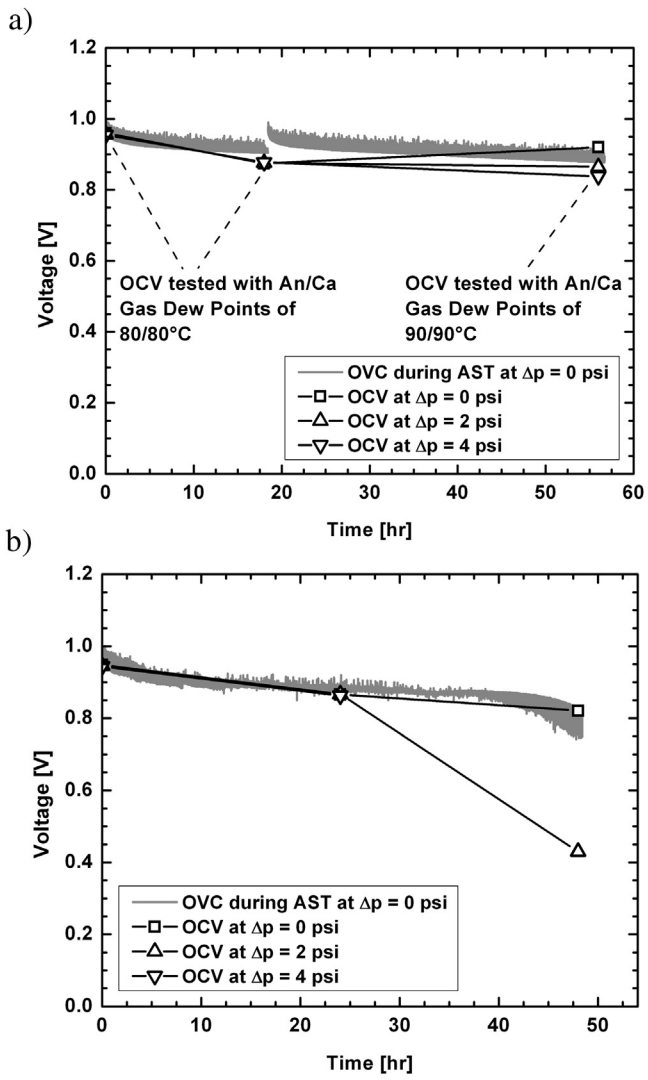

Fig. 6. OCV degradation and OCV at select H_2/air differential pressures of (a) pristine MEA and (b) MEA containing a defect.

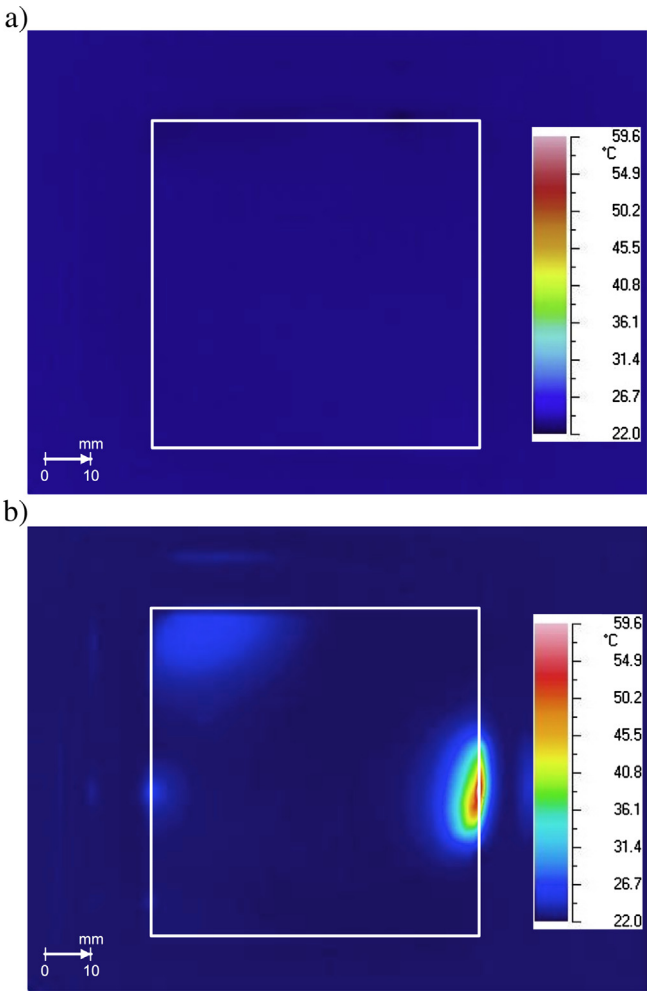

Fig. 7. IR thermography on pristine MEA after (a) 18 and (b) 56 h of exposure to AST.

area is exposed to large stresses during the hot press process and in the standard single cell assembly method used here, it is neither mechanically protected by the catalyst layer/GDL assembly, nor by the gasket. Thus, for the employed assembly method, the location of the hole at the edge of the active area was part of the structurally weakest area in the MEA/gasket assembly.

Fig. 8 shows IR thermography results for an MEA that contained a 2 cm^2 defect after exposure to 48 h of aging via AST. The temperature range of the data spans from 22.6 to 34 °C. The figure further shows the outline of the active area of the MEA and the known location and outline of the catalyst defect. The data indicated that the selected AST resulted in rapid degradation of the MEA at three locations: (i) at the transition of catalyst/GDL area to gasket area, (ii) inside the catalyst area in the upper right corner of the active area, and (iii) at the circumference of the introduced defect. These locations represent three different mechanical support structures: (i) thin area of potentially exposed membrane, (ii) complete catalyst layer/GDL assembly, and (iii) the transition of catalyst coated to uncoated area beneath the GDL, respectively. The advanced degradation of the MEA in all of these areas implied that the selected AST was very effective in aging the MEA. In fact, it was so effective that it prevented the identification of the area that was most prone to developing a failure point, i.e., that developed the failure point first. More studies using a less rapid AST procedure are required to study the onset of failure point development in PEMFC.

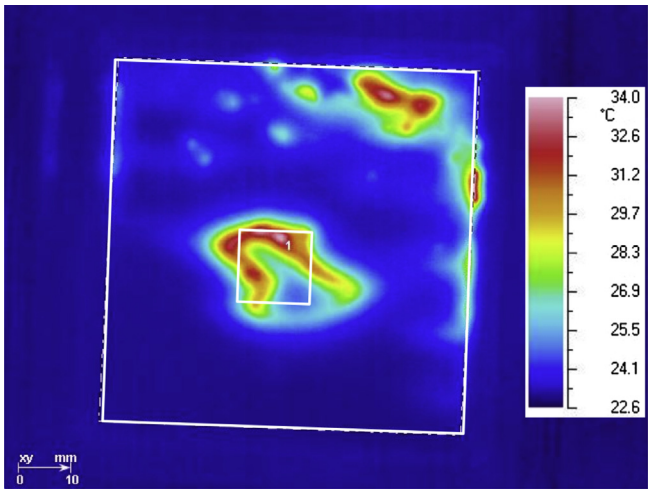

Fig. 8. IR thermography on MEA containing defect after failure induced by AST. Active area of MEA and location of defect are indicated by white lines.

5. Summary and conclusions

A novel single cell hardware and methodology was developed that enabled the spatial detection of pinholes and failure points in PEMFC in a quasi in-situ experiment. The system was based on performing IR thermography on crossover hydrogen reacting with ambient air. The method divided the operation of the fuel cell into two distinct phases: (i) operation/aging of the cell in *fuel cell configuration* and (ii) spatial, high resolution detection of increased hydrogen crossover in *IR configuration*. The new hardware was successfully employed to detect and localize failure points in pristine MEAs, as well as MEAs that contained defects. The results provided evidence that the unprotected MEA at the GDL to gasket interface is an area prone to the development of failure points, which as Sompalli et al. have shown may also be related to the alignment of the anode and cathode electrodes with each other [21]. It further suggested that a 100% reduction of the catalyst loading in a specific area may trigger the development of failure points at this location. Future work will include the refinement of AST parameters in such a way that the influence of the defect on MEA lifetime can be distinguished. The objective of this work will be to determine the onset of failure point development in MEAs in the presence of a variety of catalyst coating defects.

Acknowledgments

We gratefully acknowledge the U.S. Department of Energy under subcontract number DE-AC36-08-GO28308 for funding this work. We would also like to acknowledge M. Yandrasits and G. Haugen from 3M for fruitful discussions on IR based in-situ fuel cell diagnostics, and R. Mukundan from Los Alamos National Laboratory for advice on AST related topics.

References

[1] R. Borup, et al., Chem. Rev. 107 (10) (2007) 3904–3951.
[2] M.M. Mench, E.C. Kumbur, T.N. Veziroğlu, Polymer Electrolyte Fuel Cell Degradation, Academic Press, Amsterdam; Boston, 2012, p. xi, 460 pp.
[3] T. Uchiyama, M. Kato, T. Yoshida, J. Power Sources 206 (2012) 37–46.
[4] F. Ettingshausen, et al., J. Power Sources 194 (2) (2009) 899–907.
[5] X.Z. Yuan, et al., J. Power Sources 205 (2012) 324–334.
[6] X.Z. Yuan, et al., J. Power Sources 195 (22) (2010) 7594–7599.
[7] S.S. Zhang, et al., J. Power Sources 205 (2012) 290–300.
[8] X.Z. Yuan, et al., J. Power Sources 196 (22) (2011) 9107–9116.
[9] H. Czichos, Handbook of Technical Diagnostics: Fundamentals and Application to Structures and Systems, Springer, 2012.
[10] M.W. Murphy, B.A. Litteer, Method for Detecting Electrical Defects in Membrane Electrode Assemblies, General Motors Corporation, USA, 2004.
[11] S.B. Roscoe, et al., Fuel Cell Performance Monitoring by Optical Infrared Thermography, 3M Innovative Properties Company, USA, 2006, p. 14.
[12] G.J. Lamont, D.P. Wilkinson, Method and Apparatus for Detecting and Locating Perforations in Membranes Employed in Electrochemical Cells, Ballard Power Systems Inc., Canada, 1998, p. 30.
[13] N.V. Aieta, et al., J. Power Sources 211 (2012) 4–11.
[14] N.V. Aieta, et al., Abstracts of Papers of the American Chemical Society, vol. 242, 2011.
[15] M. Ulsh, et al., ECS Trans. 50 (2) (2012) 919–926.
[16] H.H. Wang, X.-Z. Yuan, H. Li, in: PEM Fuel Cell Durability Handbook, CRC Press/Taylor & Francis, Boca Raton, FL, 2012, p. xix, 558 pp.
[17] S. Kundu, et al., J. Power Sources 182 (1) (2008) 254–258.
[18] S. Kundu, et al., J. Power Sources 183 (2) (2008) 619–628.
[19] A. Ohma, et al., J. Electrochem. Soc. 154 (8) (2007) B757–B760.
[20] K. Teranishi, et al., Electrochem. Solid State Lett. 9 (10) (2006) A475–A477.
[21] B. Sompalli, et al., J. Electrochem. Soc. 154 (12) (2007) B1349–B1357.